ELSEVIER

Polymer 41 (2000) 8075–8082

polymer

www.elsevier.nl/locate/polymer

Material homogeneity and structural dynamics in polymer–electrolyte composite microparticles

J.V. Ford, B.G. Sumpter, D.W. Noid, M.D. Barnes*

Chemical and Analytical Sciences Division, MS 6142, Oak Ridge National Lab., P.O. Box 2008, Bldg. 4500S, Oak Ridge, TN 37831-6142, USA

Received 16 November 1999; received in revised form 17 February 2000; accepted 17 February 2000

Abstract

We describe optical diffraction, or 2D angle-resolved light scattering, measurements for probing structure and morphological dynamics of isolated poly(ethylene glycol) (PEG) microparticles doped with NaCl or $CaCl_2$. Of specific interest was the effect of dopant salt concentration and polymer host molecular weight on composite microparticle homogeneity (phase-separation behavior) and evaporation dynamics determined from changes in both microparticle size and refractive index with time. In general the drying rate was higher for microparticles doped with $CaCl_2$, and only in the case of $CaCl_2$ doped microparticles was PEG molecular weight found to effect the drying rate. Furthermore, $CaCl_2$ doped microparticles had a higher concentration threshold with regard to homogeneity when compared with NaCl doped microparticles. The results are discussed in terms of the known structures for monovalent electrolytes doped into PEG thin films and polymer-like oligomers in the gas phase, and on possible modifications of these structures due to differences in the intermolecular interactions of the two cationic species with the residual solvent and the polymer matrix.

Keywords: Polymer composite; Polymer electrolyte; Poly(ethylene glycol)

1. Introduction

The quest for new materials as energy storage devices for the rechargeable battery industry has led researchers over the last 20 years to study a wide variety of solid polymer electrolytes (SPEs). As early as 1967, the complexing properties of poly(ethylene glycol) (PEG) were elucidated [1]. Wright and coworkers [2,3] in 1973 began studying the conducting properties of PEG doped with inorganic salts of sodium and potassium, which led to a wide variety of polymer/inorganic salt studies [4]. The interest in these materials evolved from simple formulation of new materials with increased conductivity to the determination of the structure of these materials in thin films and melts. However, as yet only a limited number of polymer-to-salt ratios have been reported. In this paper we apply an optical diffraction method to explore the effect of electrolyte dopants (NaCl and $CaCl_2$) in isolated PEG microparticles. These experiments were designed to explore the effects of dopant identity, dopant concentration, and polymer molecular weight on material homogeneity, as well as microparticle drying kinetics and dielectric constant.

For composite microparticles, material homogeneity, dielectric constant and drying rate were determined by the interactions between the residual solvent (water), the electrolyte dopant, and the polymer matrix. In order to gain insight into these interactions an understanding of previous work on SPE thin films and gas-phase analogs of the polymer–electrolyte composites was required. The basic crystalline structure of PEG is a helix composed of seven monomer units making two turns [5–7]. However, solid PEG is not completely crystalline, there is a significant portion in an amorphous state. The first polymer electrolyte crystalline structure elucidated for SPE thin films was also helical. In this case six monomer units formed a helix making one turn. The metal cation took up positions within the turn of the helix with the anionic species located external to the lattice, but still coordinated to the cation [8,9]. This structure has been applied to most of the polymer electrolytes where the number of ether oxygens available for complexation with the cation (the EO/C ratio) was is between 1:1 and 4:1. A second structure was determined for an EO/C ratio of 6:1. Two chains interact forming a half cylinder, two half cylinders then merge forming a cylindrical tube. The cation resides within the tube, while the anions are located exterior

* Corresponding author. Tel.: + 1-423-574-4923; fax: + 1-423-574-8363.

E-mail address: nmz@ornl.gov (M.D. Barnes).

0032-3861/00/$ - see front matter
PII: S0032-3861(00)00161-0

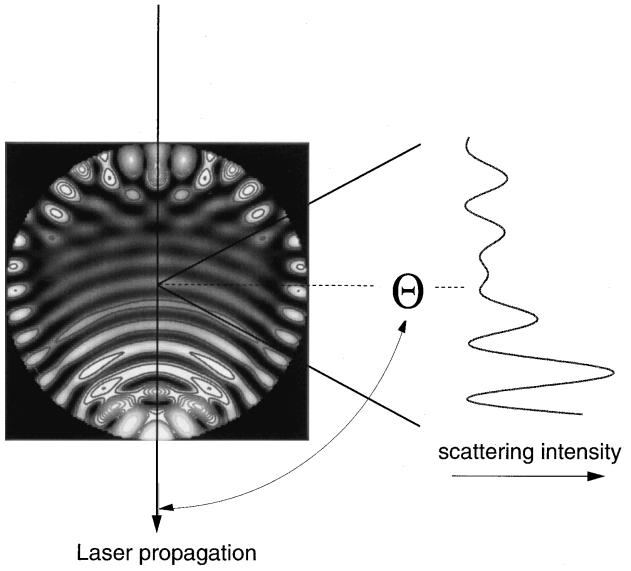

Fig. 1. Calculated internal intensity distribution for a 3 μm homogeneous sphere. The right hand vertical graph shows angular scattering in 1D along the 0° polar angle. Θ is the azimuthal or scattering angle and is located in the plane of the figure. The polar angle is measured perpendicular to the plane of the figure.

to the cylinder and are unable to coordinate with the cation [10]. In addition, recent work on melts and aqueous PEG, which are considered amorphous, indicate a short range order similar to the crystalline helical structure [11,12].

Although not commonly used for polymer characterization, matrix assisted laser desorption and ionization (MALDI) was used to study a few polymer electrolyte systems. This work studied small oligomers with alkali metal charge centers, in order to gain an understanding of the decay mechanism of the polymer/cation complex [13] and to determine the gas phase structure of the polymer/cation complex [14,15]. The gas phase structure observed had the cation enfolded by the polymeric material. This structure or 'kernel' forms a solvation sphere, which maximized the interactions between the ether oxygens of the polymer and the cation. The structure of the 'kernel' was independent of polymer size. In mass spectrometric studies there no counter-ion effects. It is interesting to note that the helical structure of the PEG/cation complex found in thin films are generally very similar to the gas-phase results.

A rapidly growing area of materials science is the creation and characterization of materials on the meso and nanoscale. Of particular interest are composite materials. Recent work in our laboratory has focused on examining the chemistry of ultra small volumes using optical methods. Combining optical interrogation with electrodynamic trapping we have examined dielectric properties and phase separation of bulk immiscible polymer blended microparticles [16,17], detected single molecules in microdroplets [18–20], and monitored interesting structural dynamics in polymer–electrolytes [21]. Furthermore, Esen et al. [22] have used photoinitiated polymerization to create polymer microparticles in an electrodynamic trap, which were then characterized optically.

In this paper, 2D optical diffraction was used to probe electrodynamically trapped polymer–electrolyte composite microparticles. Fig. 1 shows the physical basis of this measurement. When a spherical dielectric particle is illuminated with plane-polarized radiation, a highly non-uniform intensity distribution within the particle is produced by interference between refracted and internally reflected rays. The node structure of the intensity distribution has an angular frequency and envelope pattern, which is highly sensitive to microparticle size and refractive index. Experimentally, the angular intensity pattern is mapped in the far field using a multichannel detector to detect scattering intensity for both azimuthal (scattering) and polar angles. In Fig. 1, Θ marks the azimuthal angle, which lies in the plane of the figure, and is centered perpendicular to the laser axis. The polar angle would be located perpendicular to the plane of the figure. Intensity data along the polar angle allows the onset of material inhomogeneity to be determined unambiguously since homogeneous particles have Gaussian intensity fluctuations along a given polar angle. Experimentally, this means that a given diffraction fringe has the same intensity at all points. Therefore, the observation of low frequency or non-Gaussian intensity fluctuations along the polar angle indicates that a microparticle is inhomogeneous. Intensity variations are the result of scattering or phase distortions caused by regions (subdomains) within the microparticle where the local refractive index is different from that of the host material.

Recently, we examined the effects of subdomain size, refractive index and number density both experimentally and theoretically [23]. Visibility of subdomains was related to their scattering efficiency, which scaled as

$$\frac{d^3}{\lambda^2}\left|\frac{m^2-1}{m^2+1}\right| \tag{1}$$

where d was the diameter of the subdomain, λ was the illumination wavelength, and m was the relative refractive index defined as $n_{\text{domain}}/n_{\text{host}}$. It was found that when Eq. (1) was ≈ 0.025, subdomains caused observable fringe distortion in experimental 2D diffraction patterns. Therefore, for a given number of scatterers, as m approaches 1 the subdomain size (d) must increase for fringe distortion to be observed.

Electrodynamically trapped polymer composite microparticles composed of PEG doped with either NaCl or $CaCl_2$, at polymer-to-salt (P/S) ratios ranging from >50:1 to ~1:90 (by weight) were probed using 2D optical diffraction. For this range of P/S ratios, the corresponding EO/C ratios are in the range of >86:1 to ~1:30. Examination of intensity profiles along given polar angles (i.e. along a diffraction fringe) of the experimental optical diffraction patterns were used to determine microparticle homogeneity. The homogeneity data for the two dopants provided insight

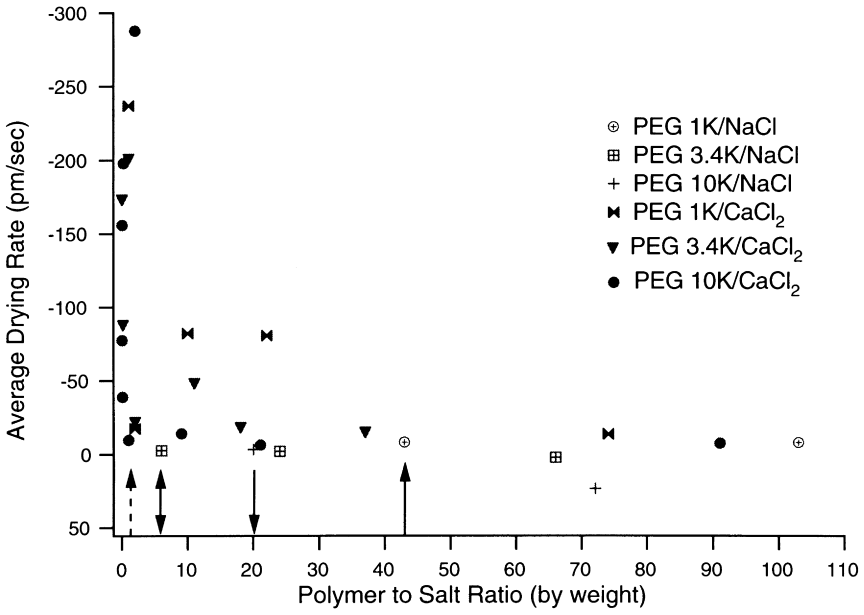

Fig. 2. Summary of drying rates and homogeneity thresholds for PEG microparticles doped with either NaCl or $CaCl_2$. The homogeneity threshold marks the lowest polymer to salt (P/S) ratio where the polymer/electrolyte microparticle was homogeneous. Homogeneity thresholds are marked with arrows: ↑ for PEG 1K with NaCl, ↕ for PEG 3.4K with NaCl, ↓ for PEG 10K with NaCl, and ⇑ for PEG 1K with $CaCl_2$. PEG 3.4K and 10K do not have a homogeneity threshold. A positive drying rate indicates a size increase or particle growth.

into possible structures within the microparticle, which should be similar to known gas phase and thin film structures for analogous PEG based polymer-electrolytes. For homogeneous microparticles, quantitative comparison of angular scattering data with Mie theory calculations resulted in direct assignment of microparticle size and refractive index. Using a timed sequence of 2D angular scattering patterns, the evaporative dynamics of the composite systems were determined.

2. Experimental

Polymer/electrolyte microparticles were produced on-demand from aqueous droplets and levitated in an electrodynamic trap. A HeNe laser (632.8 nm) polarized perpendicular to the scattering plane was used as an illumination source. Details of the experimental apparatus, optical setup and calibration procedures for correlating CCD pixel to optical scattering angle have been presented elsewhere [20,24].

Aqueous polymer stock solutions were prepared using PEG with average molecular weights of 1000 (PEG 1K), 3400 (PEG 3.4K) and 10,000 (PEG 10K) amu (Aldrich) in 250 ml batches at weight percents from 1 to 1.35%. The polymer/electrolyte solutions were formulated by mixing a known weight of the PEG stock solution and either sodium chloride (Fisher Scientific) or anhydrous calcium chloride (Mallinckrodt). All reagents were used without additional purification or drying and stock solutions were prepared using water generated from a Nanopure (Barnstead/Thermolyne) water system.

Microdroplets were generated on demand using a home-built piezoelectric droplet generator [19], following loading of the polymer–electrolyte solution into a Pyrex tip through vacuum aspiration. The tip was cleaned between each polymer/electrolyte system to insure that contamination between systems did not occur. Rapid solvent evaporation occurred during the first few hundred milliseconds after droplet ejection, resulting in a relatively dry microparticle (typically 5–20% residual solvent). The amount of residual solvent was dependent on ambient conditions within the trap, determined by laboratory temperature and relative humidity. For observation times on the order of seconds, evaporation of residual solvent from microparticles was observable as a reduction in microparticle diameter with a concomitant increase in refractive index.

The particle trap used has a three-electrode geometry [5,9] with a 60 Hz AC voltage (~350 V) applied to the ring electrode. The endcaps were biased with a small DC voltage to offset gravitational forces. An induction electrode located above the trap was biased at ~400 V to increase the charge to mass ratio of the microparticle to improve trapping efficiency. The scattering angle, as determined by calibration, was 90.964 ± 19.40° with respect to the direction of laser propagation. The detection angle was defined geometrically by the *f*/1.5 collection objective, and the collimated light was spatially filtered and reduced in size to match the dimensions of the CCD chip. The CCD camera (Spectra Source Instruments) was thermoelectrically cooled, and digitized at 16 bits.

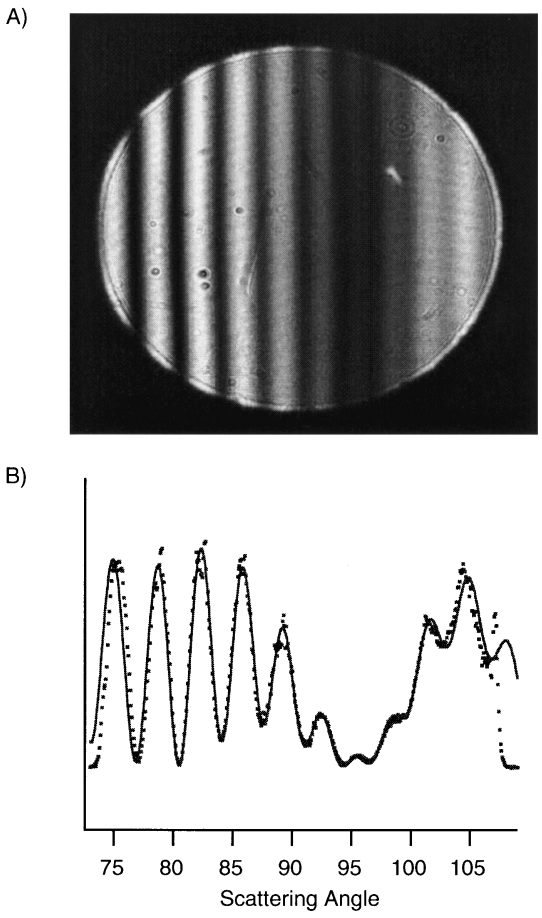

Fig. 3. (A) 2D optical diffraction pattern from a homogeneous microparticle composed of PEG 3.4K doped with $CaCl_2$ with a polymer to salt ratio (P/S) of 1:1 (by weight). (B) Comparison of a 1D slice, at the zero polar angle in the 2D pattern shown in part (A), and Mie theory calculations. The experimental data is shown as dots (●) and Mie calculations are shown as a solid line (—). The excellent agreement between the experimental data and the Mie calculations is a hallmark of homogeneous microparticles. The microparticle has a diameter of 10.952 ± 0.005 μm with a refractive index of 1.4575 ± 0.0005.

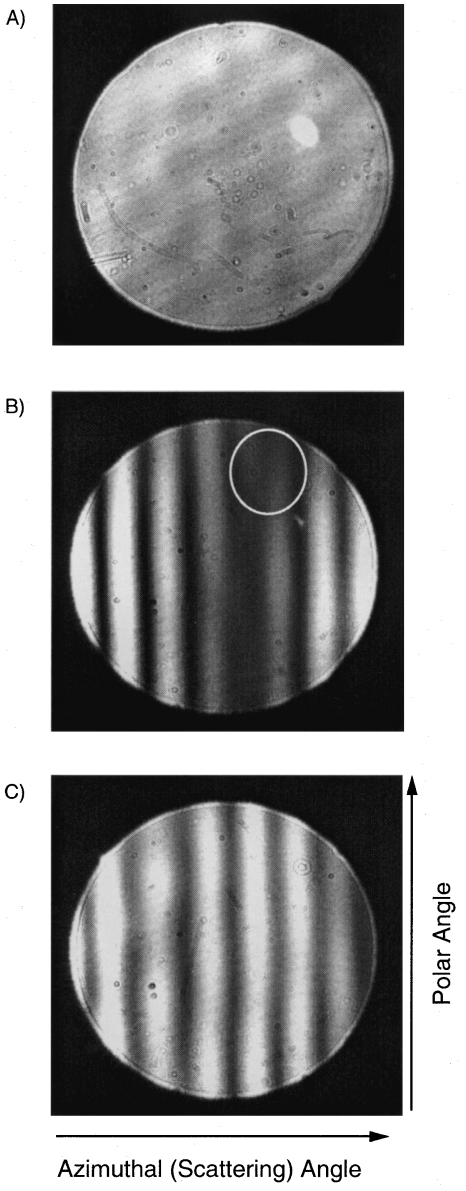

Fig. 4. 2D optical diffraction patterns obtained from inhomogeneous microparticles. (A) Complete absence of diffraction fringes. The system is PEG 1K doped with NaCl at a polymer to salt ratio (P/S) of 1:25. (B) A clear diffraction pattern with intensity voids. The system is PEG 10K with NaCl at a P/S ratio of 1:45. (C) A clear diffraction pattern, however the intensity variations along the vertical fringes are non-uniform. The system is PEG 10K with NaCl at a P/S ratio of 1:45.

2D diffraction patterns obtained were stored and 1D horizontal slices (1D phase functions) corresponding to the 0° polar angle were generated. Comparison of the experimental 1D phase functions with 1D phase functions calculated using Mie theory was performed by minimizing a predefined error parameter (chi) [17]. The size and refractive index from the Mie theory calculations, at minimum chi, was assigned to the microparticle. Particle size and refractive index were determined for homogeneous microparticles with absolute errors of ±0.005 μm and ±0.0005, respectively. This comparative process yields quantitative results for microparticles with diameters in the range of 3–20 μm. Furthermore, if the composite microparticles examined were not spherical, to ~1 part in 10^5, the comparison between theory and experiment would result in large error values. Evaporative dynamics were determined by taking a series of 2D angular scattering patterns at fixed time intervals. The minimum number of observation in each series was ~30 with a typical time step of 2 min. A minimum of two and a maximum of 12 microparticles were examined for each P/S ratio.

3. Results and discussion

The primary goal of this work was utilization of 2D angular scattering to probe the effect of electrolyte dopants on material homogeneity, microparticle drying rate, and dielectric constant in isolated polymer electrolyte composite

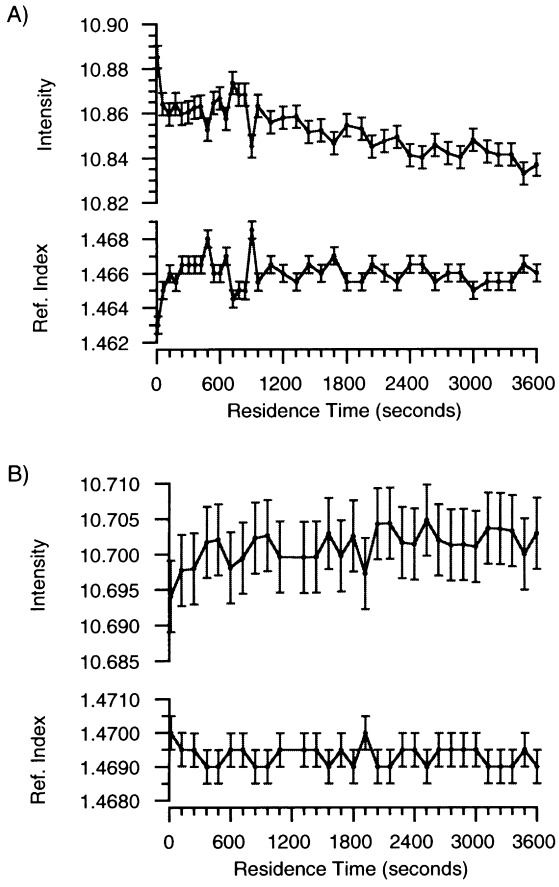

Fig. 5. Graphs of size and refractive index versus microparticle residence time in the electrodynamic trap for (A) a drying microparticle (PEG 1K/$CaCl_2$ with a P/S ratio of 74:1), and (B) a microparticle experiencing size growth (PEG 3.4K/NaCl with a P/S ratio of 66:1). The error bars shown for the size and refractive index measurements are ± 0.005 μm and ± 0.0005, respectively.

microparticles. Fig. 2 shows the average drying rates and homogeneity threshold salt concentrations as a function of weight ratio for microparticles doped with NaCl and $CaCl_2$. The vertical arrows in Fig. 2 highlight the lowest P/S ratio for the formation of homogeneous microparticles, hereafter referred to as the homogeneity threshold. There is no homogeneity threshold (all the microparticles examined were homogeneous) for PEG 10K doped with $CaCl_2$. Furthermore, only microparticles at two P/S ratios (1:5 and 1:44) were inhomogeneous for PEG 3.4K/$CaCl_2$ composites. Fig. 3A shows a 2D diffraction pattern for a homogeneous microparticle of PEG doped with $CaCl_2$. As shown in Fig. 3B, the quantitative agreement between Mie theory and a 1D slice of the experimental diffraction pattern indicated that the microparticle was both homogeneous and spherical. Fig. 4 shows some typical 2D angular scattering patterns obtained from inhomogeneous microparticles. Microparticle heterogeneity was signaled by fringe distortion in the experimental diffraction pattern. At low subdomain concentrations, the effect was usually observed as low frequency intensity oscillations along diffraction fringes (i.e. along the polar angle) that are otherwise well defined (Fig. 4C). At higher dopant concentrations disruptions in a well-defined diffraction pattern may be observed as voids (Fig. 4B) or waves and in the extreme case a complete loss of fringe contrast (Fig. 4A).

The average drying rate, for homogeneous composite microparticles, was calculated by taking the overall size change divided by the residence time. A negative drying rate corresponds to a decrease in particle size, and a positive drying rate corresponds to an increase in particle size. Typically, size and refractive index are anti-correlated. Fig. 5A illustrates a typical size and refractive index responses for a microparticle undergoing slow evaporation (PEG 1K/$CaCl_2$ with a P/S ratio of 74:1). Fig. 5B illustrates the size and refractive index responses for microparticles undergoing a size increase (PEG 3.4K/NaCl with a P/S ratio of 66:1).

Assuming partial molar volumes are additive the refractive index can be expressed in terms of the contributions from the dopant (crystalline form), the PEG host and water according to the following relation [24]:

$$n_{\text{exp}} = \left(\frac{V_{\text{salt}}}{V_{\text{particle}}}\right) n_{\text{salt}} + \left(\frac{V_{\text{PEG}}}{V_{\text{particle}}}\right) n_{\text{PEG}} + \left(\frac{V_{\text{water}}}{V_{\text{particle}}}\right) n_{\text{water}} \quad (2)$$

where n is the refractive index and V is volume. Eq. (1) is valid in the limit where the electrolyte is present as crystalline subdomains ($d > 63$ nm for NaCl and $d > 60$ nm for $CaCl_2$) within the microparticle. When the electrolyte is completely dissociated, as is the case in an aqueous environment, Eq. (1) is modified by eliminating the first term and modifying the refractive index of the second and third term to account for the role of the ions in the microparticle. The refractive indices reported in the CRC for aqueous solutions of NaCl and $CaCl_2$ [25] could be used for the residual water, however, the loss of residual solvent (drying) would result in a salt solution of increasing concentration and therefore a variable refractive index during the course of the experiment. More importantly, changes in refractive index of the PEG host material upon complexation of a cation are unknown at this time. As a qualitative approach, the following discussions will assume that the refractive indices of the PEG host and the residual water were constant. Therefore, changes in the experimental refractive index are discussed in terms of loss of residual water.

Examination of the data shown in Fig. 2 reveals two points of interest: (1) The PEG/NaCl system had two instances (occurring for P/S ratios of 66:1 and 72:1 for PEG 3.4K and 10K, respectively) in which the microparticle actually undergoes a size increase, evidenced by a positive drying rate and a concomitant decrease in the refractive index, and (2) generally, the drying rates for PEG/$CaCl_2$ systems are significantly larger than the drying rates obtained for PEG/NaCl systems at similar P/S ratios.

Experimental results suggested that microparticles with a positive drying rate appear to reintegrate water into the microparticle, as evidenced by a reduction in the refractive

index. Complexation of the dissociated ions within the microparticle occurs in two ways: either solvation by water or coordination by the polymer chains. The differences between drying rates for $CaCl_2$ and NaCl doped microparticles may be explained in terms of the increased number of ions needing to be complexed and the increased strength of the intermolecular interactions within the microparticle. For example, the ion–dipole interactions between Ca^{2+} and water are much stronger than interactions between Na^+ and water. In addition, it is also expected that the interaction between the cation and the polymer matrix increase with the cationic charge. Preliminary ab initio calculations at the Hartree–Fock level give binding energies for Ca^{2+} that are approximately four times larger than for Na^+. Both the cationic charge and the total number of ions in a given microparticle was larger for $CaCl_2$ doped systems, therefore a higher residual water content was needed to meet ion solvation requirements. This argument was supported by the fact that the number of ether oxygens available for cationic complexation was relatively constant for all PEG molecular weights. Therefore, in order to increase the number of coordinating species, retention of water must have occurred. What is not completely understood is why the water initially retained for ion solvation was released during the experimental run. Two complementary processes are speculated to occur within the microparticle allowing the observed drying to occur. First, the ions are initially solvated to the maximum extent, as is the polymer matrix since water is the predominant species. As drying occurs, water is removed from the solvation shells of the ions, reducing the degree of solvation. Secondly, as the degree of solvation is reduced, interactions between the partially solvated ions increase, as does interactions between the cations and the polymer matrix. It was likely that PEG/cation complexation had already occurred in solution, so during evaporation only the extent of complexation increased. The drying rate data clearly supports this assertion since $CaCl_2$ doped systems have much higher drying rates.

As seen in Fig. 2, two different PEG/NaCl microparticles do not dry, instead over the course of the observation time window the microparticles grew in size. It is not completely understood why PEG 3.4K/NaCl (P/S ratio of 66:1) undergoes a size increase, albeit a small one (refer to Fig. 5). The refractive index may indicate that water was absorbed onto the microparticle. For PEG 10K/NaCl microparticles with at a P/S ratio of 72:1, there is another explanation for the particle growth observed. For this system, microparticles undergo size oscillations, which have been described previously [21]. Briefly, the complexation of Na^+ by individual polymer chains within the PEG matrix resulted in a local structural change. The structure change was propagated along or between chains by the movement of the cation resulting in expansion and contraction of the microparticle. This size oscillation phenomenon was also observed for PEG 10K/NaCl with a P/S ratio of 20:1, which exhibited an overall size decrease and a negative drying rate. Because of the oscillatory nature of these two systems the sign of the drying rate actually specifies where in the size oscillation the experimental observations ceased.

The issue of cationic complexation by the polymer matrix was essential in explaining the electrolyte concentration dependence of the homogeneity threshold. As seen in Fig. 2, there was a significant difference in the ability of PEG to mix homogeneously with NaCl and $CaCl_2$. PEG/$CaCl_2$ composites are homogeneous at much higher salt concentrations when compared to PEG/NaCl composites. In addition, when PEG/$CaCl_2$ microparticles were inhomogeneous, they typically had clear diffraction patterns with poor fringe contrast. On the other hand, inhomogeneous microparticles of PEG/NaCl typically had no discernible fringe structure other than for PEG 10K/NaCl at P/S ratios of 8:1, 2:1, 1:1, and 1:45 (saturated). In these instances, the microparticles examined exhibited a change from a relatively well-defined diffraction pattern, with poor fringe contrast or voids, to a pattern that was undefined and random. In general, the change occurred during the first few minutes of the experiment ($<$15 min) indicating that there was a significant structural change within the microparticle. Comparisons of the homogeneity thresholds for microparticles doped with NaCl indicated that polymer molecular weight played a minor role in the mixing of the dopant and the polymer matrix. However, in the case of PEG 10K the fact that most of the inhomogeneous particles initially exhibited some identifiable fringe structure may indicate that mixing within this system was initially more uniform. On the other hand, $CaCl_2$ doped microparticles exhibited a clear difference in homogeneity threshold for the three molecular weights of PEG. As the molecular weight of the polymer matrix increased, homogeneous microparticles could be formed at high salt concentrations. This is especially true for PEG 10K, although the differences in homogeneity threshold are minor for PEG 3.4K and PEG 10K, since only two P/S ratios (1:5 and 1:44) are inhomogeneous in the PEG 3.4K matrix. Examination of the refractive indices for the PEG/$CaCl_2$ microparticles indicated that material homogeneity was correlated to the residual water content of the microparticle, since with few exceptions the microparticle refractive index was lower than the pure PEG value (1.4717). In two instances where the refractive index was higher than 1.4717, the value was only slightly higher which as yet has no straightforward explanation, but could be caused by the presence of nanocrystalline subdomains or modification of the PEG refractive index upon complexation of the cation.

The differences between inhomogeneous microparticles of PEG/$CaCl_2$ and PEG/NaCl indicated that the subdomains within the microparticle resulting in inhomogeneity could have had a dramatically different size, refractive index and/or number density. As determined in Ref. [23], the combination of subdomain size and refractive index determine whether material inhomogeneity will be detected, and the number density of the subdomains determines the extent of

distortion observed in 2D optical diffraction patterns. Since the dopants were both simple inorganic salts the subdomains present were expected to be structurally similar. Two possible subdomain types were salt nanocrystallites and/or PEG/cation complexes. Since the cations used are analogous to those used in thin polymer–electrolyte films and gas phase studies, the subdomains present were probably helical, with the cation complexed by the ether oxygens of the PEG matrix.

Considering the presence of salt nanoscrystallite subdomains, it was important to realize that the presence of such subdomains would increase the refractive index measured for the microparticle since the bulk refractive indices of the salt dopants (NaCl = 1.54 and $CaCl_2$ = 1.52) are higher than that of pure PEG (1.4717). If nanocrystallite subdomains were present, and were smaller than the detection limits of the technique, the only manifestation of their presence would have been an increased refractive index. On the other hand, if the dimensions of the subdomains exceeded ~60 nm the microparticle will appear inhomogeneous. It was unlikely, however, that a significant amount of residual water and microcrystalline salt subdomains could coexist. Therefore, while it was impossible to rule out the presence of crystalline salt subdomains, PEG/cation complexes were probably the predominant subdomains within the microparticle. This assertion was supported by the fact that with only two exceptions, the composite microparticles examined exhibited a refractive index lower than the pure PEG value.

Since the dominant subdomain was most likely composed of a PEG/cation complex, why does the NaCl dopant have such a low homogeneity threshold? Thin film literature indicated that PEG incorporates monovalent cations into the turns of the helix, resulting in a conformational change of the matrix. In addition, work on thin films composed of δ-$MgCl_2$ and PEG (400 amu) exhibited helical structures similar to those obtained for the alkali metal cations in thin films. Moreover, as the salt concentration increased, complexation also occurred at the hydroxyl end groups [26]. Residual water competes with the complexation interaction between the cation and the polymer matrix. It was speculated that this competition was the key to understanding the homogeneity threshold data. Water solvation mediated the complexation of the cation by the PEG matrix in two ways: (1) the presence of solvent molecules about the cation resulted in a species unable to fit into the turns of the PEG helix, a steric effect, eliminating formation of PEG/cation complexes; and (2) if PEG/cations complexation occurred, the presence of water reduced the number of ether–oxygen interactions, and therefore the conformational change associated with complex formation did not occur. Since, $CaCl_2$ doped PEG microparticles retained significantly more water than NaCl doped PEG, the complexation of the Ca^{2+} by the PEG matrix was reduced, which either reduced the number or size of the subdomains within the microparticle. Consequently, the microparticles had high contrast 2D optical diffraction pattern indicative of a homogeneous microparticle.

4. Summary

This study probed the effects of dopant identity, dopant concentration, and polymer host molecular weight for microparticles composed of PEG doped with either NaCl or $CaCl_2$, utilizing 2D optical diffraction. Dopant identity played a role in both drying rate and homogeneity threshold. The fact that inhomogeneous polymer–electrolyte microparticles were formed may indicate that the SPE thin films could also have small subdomains on the macromolecular length scale. Only in the case of $CaCl_2$ doping of PEG microparticles were effects correlated to dopant concentration and polymer molecular weight. The primary explanation of the homogeneity threshold and drying rate data was based on the structural data elucidated for PEG/cation complexes found in the gas phase and analogous SPE thin films, which indicated that cations intercalated into a helical PEG matrix inducing a conformational change. Consequently, formation of a PEG/cation complex resulted in a subdomain within the microparticle. Subdomain formation was mediated by the presence of residual water. It was speculated that residual water hindered the ability of the PEG matrix to complex cationic species due to solvation shells around the cation. If PEG/cation complexes were formed, the presence of residual water did not allow the PEG matrix and the cation to complex completely reducing or eliminating the conformational change typically associated with PEG/cation complex formation. This hypothesis explained the homogeneity threshold data and drying rate results for NaCl and $CaCl_2$, which clearly indicated that the homogeneity threshold was higher for $CaCl_2$ as were drying rates which are indicative of a high residual water content within the microparticle. It should be noted that the anion plays an important role in determining the residual water content within the microparticle, due to solvation constraints. In order to gain additional insight in polymer composite materials, two-color interrogation is planned to better determine the exact composition of ternary microparticles.

Acknowledgements

This research was sponsored by Office of Basic Energy Sciences, Divisions of Chemical and Material Sciences, US Department of Energy, under Contract DE-AC05-96OR22464 with Oak Ridge National Laboratory, managed by Lockheed Martin Energy Research Corporation. J.V.F. acknowledges support from the ORNL Postdoctoral Research Associates Program administered by Oak Ridge Associated Universities.

References

[1] Shatenstein AI, Petroc ES, Yakovleve EA. J Polym Sci C 1967;16:1799.
[2] Fenton DE, Parker JM, Wright PV. Polymer 1973;14:589.
[3] Wright PV. Br Polym J 1975;7:319.
[4] Vincent CA, MacCallum JR, editors. Polymer Electrolyte Reviews, vols. 1 and 2. London: Elsevier, 1987–1989 (and references therein).
[5] Takahashi Y, Tadokoro H. Macromolecules 1973;6:672.
[6] Russell TP, Ito H. Macromolecules 1988;21:1703.
[7] Kugler J, Fischer EW, Peuscher M, Eisenbach CD. Makromol Chem 1983;184:2325.
[8] Chatani Y, Fujii Y, Takayanagi T, Honma A. Polymer 1990;31:2238.
[9] Croce F, Appetecchi GB, Persi L, Scrosati B. Nature 1998;394:458.
[10] MacGlashan GS, Andreev YG, Bruce PG. Nature 1999;398:792.
[11] Johnson JA, Saboungi ML, Price DL, Ansell S, Russell TP, Halley JW, Nielsen B. J Chem Phys 1998;109:7005.
[12] Branca C, Magazù S, Maisano G, Migliardo P, Villari V. J Phys Condens Matter 1998;10:10 141.
[13] Shelby TC, Wesdemiotis C, Lattimer RP. J Am Soc Mass Spectrom 1994;5:1081.
[14] von Helden G, Wyttenbach T, Bowers MT. Science 1995;267:1483.
[15] Wyttenbach T, von Helden G, Bowers MT. Int J Mass Ion Process 1997;165/166:377.
[16] Barnes MD, Kung C-Y, Lermer N, Fukui K, Sumpter SG, Noid DW, Otaigbe JU. Opt Lett 1999;24:121.
[17] Barnes MD, Ng KC, Fukui K, Sumpter BG, Noid DW. Macromolecules 1999;32:7183.
[18] Barnes MD, Ng KC, Whitten WB, Ramsey JM. Anal Chem 1993;65:2360.
[19] Kung C-Y, Barnes MD, Lermer N, Whitten WB, Ramsey JM. Appl Opt 1999;38:1481.
[20] Kung C-Y, Barnes MD, Lermer N, Whitten WB, Ramsey JM. Anal Chem 1998;70:658.
[21] Ford JV, Sumpter BG, Noid DW, Barnes MD. Chem Phys Lett 2000;316:181.
[22] Esen C, Kaiser T, Borchers MA, Schweiger G. Colloid Polym Sci 1997;275P:131.
[23] Ford JV, Sumpter BG, Noid DW, Barnes MD, Hill SC, Hillis DB. J Phys Chem B 2000;104:495.
[24] Barnes MD, Lermer N, Whitten WB, Ramsey JM. Rev Sci Instrum 1997;68:2291.
[25] Weast RC, Astle MJ, editors. CRC Handbook of Chemistry and Physics, 63. Boca Raton, FL: CRC Press, 1982 (pp. D233, D261–D262).
[26] Di Noto V, Lavina S, Longo D, Vidali M. Electrochim Acta 1998;43:1225.